Chem Rev Lett 6 (2023) 166-182

Research Article

Chemical Review and Letters
journal homepage: www.chemrevlett.com
ISSN (online): 2645-4947 (print) 2676-7279

Antimicrobial/antioxidant and cytotoxicity activities of some new mercury(II) complexes

Ameneh Malekhoseini[1], Morteza Montazerozohori[1,*], Reza Naghiha[2], Esmaeel Panahi Kokhdan[3], Shiva Joohari[4]

[1] *Department of Chemistry, Yasouj University, Yasouj 7591874831, Iran*
[2] *Department of Animal Sciences, Yasouj University, Yasouj 7591874831, Iran*
[3] *Medicinal Plants Research Center, Yasuj University of Medical Sciences, Yasuj, I.R. Iran*
[4] *Department of Basic Sciences, Yasooj branch, Islamic Azad University, Yasooj, Iran.*

ARTICLE INFO`

Article history:
Received 8 March 2023
Received in revised form 19 July 2023
Accepted 19 July 2023
Available online 10 August 2023

Keywords:
Mercury(II), Schiff base, Antimicrobial/Antioxidant, Cytotoxicity, FRAP, DPPH.

ABSTRACT

In this paper, a new aprotic N_2O_2-tetradentate Schiff base ligand and its mercury complexes were synthesized with a general formula of $HgLX_2$ (X is Cl^-, Br^-, I^-, N_3^-, NO_3^- and SCN^-) and characterized by physical and spectral techniques such as IR, UV-Visible, ^1H NMR, ^{13}C NMR, ESI/MASS, molar conductivity, thermal analysis and melting point. Moreover, nanostructured $HgLI_2$ and $HgLBr_2$ complexes were also synthesized and confirmed using SEM, EDX and XRD techniques. Thermal analysis of the ligand and complexes showed that these compounds decompose in 2-3 steps. Moreover, some thermo-kinetics activation parameters of the compounds were calculated at all the thermal decomposition steps. The biological properties of synthesized compounds were tested against two gram-positive and two Gram-negative bacteria. In addition, *Aspergillus oryzae* and *Candida albicans* were selected for antifungal screening of the compounds. Further, the bactericidal effects of the compounds were depicted by SEM images of treated bacteria by the ligand and some mercury complexes. The ability of DNA cleavage of N_2O_2-tetradentate Schiff base ligand and its complexes was investigated by the agarose gel electrophoresis method. The results showed that Schiff base mercury complexes had higher antibacterial/antifungal activity as compared with the free ligand. $HgLX_2$ compounds also showed a greater ability for cleavage of DNA than free ligand. In continue, the cytotoxicity properties of the ligand and some $HgLX_2$ (X=Cl^-, Br^- and I^-) complexes were evaluated against the PC3 cancer cells line by using MTT bioassay and nitric oxide level measurement as compared with cisplatin. Finally, the antioxidant activities of the titled compounds were measured by DPPH and FRAP methods.

1. Introduction

Microorganisms present vital roles in the cycling of nutrients, animal, plant, and human health, and global concerns for agricultural and food points of views. As exclusive kinds of life in deep subsurface and extreme environments, microorganisms can be found in various ecosystems which macroscopic organisms have occupied them [1]. Although they have many benefits but they have been recognized various diseases due to the presence of bacteria, fungal, and even yeasts [2] including their effects on inflammatory bowel disease (IBD) such as Crohn's disease (CD) [3], climate changes [1], oncohematological diseases [4], infections on mouth, throat, and esophagus [5]. Herein, the smoothly treatment of above mentioned failures are a noticeable demanding. Among varies biological [6] and chemical treatments [7] of such microorganisms, using the Schiff bases are precisely a big deal that have attracted outstanding attentions leading to investigate their biological and chemical capabilities including herbicidal [8,9], antibacterial [10], antioxidant [11], antitumor [12], antimicrobial [13], antifungal [11,14], anti-inflammatory [15], antidiabetic [16], antiviral [17], antitubercular [18], electrochemical sensors [19, 20], and catalytic activities [21]. Chelating ligands based on Schiff base structures

* Corresponding author; e-mail: mmzohory@yahoo.com, mmzohori@yu.ac.ir
https://doi.org/10.22034/crl.2023.388828.1211
This work is licensed under Creative Commons license CC-BY 4.0

have special dignity in coordination chemistry [14]. They can easily attach to the diverse metal ions to form significantly stable complexes that are applicable in industrial, biochemical, environmental, analytical, and pharmaceutical usages [11, 22-25]. Moreover, it has been approved that the metal complexes bearing Schiff base ligand can be especially applied for the production of anticancer drugs [26]. A huge library of biological active Schiff base complexes containing transition metal ions such as Cu(II) [14], V(II) [27], Fe(III) [28], Mn(II) [10], Ni(II) [12], Co(II) [29], Zn [30], Sn(IV) [31], Ru(II) [32], Au(III) [33], Cr(III) [34], Cd(II) [35], and Hg(II) [36] ions have been reported. Among all, mercury(II) is a point because it dedicates diverse concepts to biology, chemistry, and engineering communities over the recent years [37]. Having diverse applications in paper, fluorescent lamps, paints, cosmetics, sensors and batteries industries [38] and ultimately worthy amalgams are highly interested [39]. According to literature survey and in continuation of our previous works [19, 20], in the current report, the biological properties of some mercury complexes of a new N_2O_2-Schiff bases (Scheme 1) have been investigated against two fungi of *Aspergillus oryzae* and *Candida albicans and* four bacteria entitled *Escherichia coli* and *Pseudomonas* (as gram negative bacteria) and *Staphylococcus aureus* and *Bacillus subtilis* (as gram positive bacteria). Also, DNA cleavage ability was investigated for all compounds.

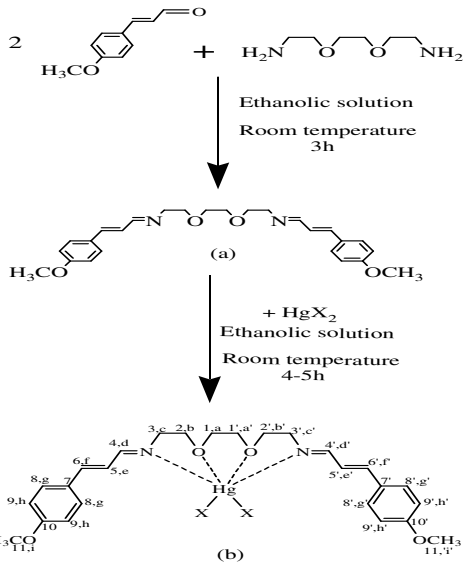

Scheme 1. The suggested structure of the free ligand (a) and $HgLX_2$(X=Cl, Br, I, SCN, N_3, NO_3) (b). The letters and numbers are used for the NMR assignment.

Eventually, the antioxidant activity (by FRAP and DPPH methods) and anticancer properties of the compounds against prostate cancer cells(PC3) were studied by MTT method and nitric oxide concentration measuring as compared with cisplatin as standard drug.

2. Experimental

2.1. Materials and Methods

Starting chemicals and solvents including of 3-(4-Methoxyphenyl)-2-propeneal, 1, 8-Diamino-3,6-dioxaoctane, KSCN, NaN_3 salts, mercury nitrate salt, HgX_2 salts (X contains chloride, bromide and iodide anions), methanol, ethanol, dichloromethane and dimethylformamide (DMF) were provided by the Merck and Aldrich companies and applied without further purification. The culture medium used for biological tests were Nutrient agar, Mueller Hinton agar (as a solid medium), and Mueller Hinton broth (as liquid culture media). *Escherichia coli* (ATCC 25922), *Pseudomonas aeruginosa* (ATCC 9027), *Staphylococcus aureus* (ATCC 6538), and *Bacillus subtilis* (ATCC 6633) were selected for antibacterial screening and *Candida albicans* and *Aspergillus oryzae* were used for antifungal tests. Infra-red (IR) spectra were recorded by FT/IR spectrometer (JASCO-680 model) in the range of 4000–400 cm^{-1} using a KBr disk. The ^1H NMR and ^{13}C NMR spectra were recorded using a Bruker DPX FT-NMR-300 spectrometer in DMSO-d_6 as solvent and tetramethylsilane (TMS) as internal standard at ambient temperature. The electronic spectra were obtained from DMF solution (2×10^{-5}M) of the compounds by JASCO-V730 spectrophotometer using a 1 cm quartz cell, in the range of 200 to 600 nm. The melting/decomposition points of the compounds were recorded by a Kruss Optronik melting point device. The molar conductivities of all compounds were measured by a Metrohm 712 conductometer in DMF solvent. Thermo-gravimetric analyses of the compounds were performed by a TGA device (STA; PerkinElmer STA6000, USA) under N_2 atmosphere with a heating rate of 20˚C/min and at temperature range of 25–1000°C. The mass spectra of the ligand and its complexes were recorded using the ESI/mass, 320ab sciex device.

2.2. Synthesis of N, N'-((ethane-1,2-diybis(oxy)) bis(ethan-2,1-diyl))bis(3-(4-methoxyphenyl)prop-2-en-1-imine) as N_2O_2 Schiff base ligand (L)

1 mmol of 1,8-Diamino-3,6-dioxaoctane was dissolved in 5 ml of ethanol and added drop wise to 2 mmol of 3-(4-Methoxyphenyl)-2-propeneal dissolved in 5ml of ethanol and then the mixture was stirred vigorously for 3h at room temperature. After 3 h, a yellow solution was obtained and then the ligand precipitated from the reaction mixture overnight. The resulting yellowish cream-colored precipitate was separated, washed with ethanol and dried at room temperature. Yield: 54.1%. M.p.: 108–112 ˚C.

2.3. Synthesis of Hg(II) complexes

To prepare the mercury complexes, an ethanolic solution of the freshly prepared N_2O_2 tetradentate ligand was

added drop by drop to the ethanolic solution of the halid/pseudohalide salts of Hg(II), and the reaction mixture was stirred vigorously for 4 to 5 h at ambient temperature. The prepared complexes were filtered and washed with cold ethanol and then dried under air at 150 ° C. Important physical and spectral data (Infrared (IR) spectra, UV-visible, ^{1}H, and ^{13}C NMR) have been collected in Tables 1- 4 based on the suggested structures in Scheme 1**.**

Table 1. Analytical and physical data of the N_2O_2-Schiff base ligand (L) and its mercury compounds after drying at 150 ° C.

Compounds	Color	Melting (decomposition) points/C	Yield, %	Elemental analysis, Experimental (Calculated)%			Λ M/Ω^{-1} cm^2 mol^{-1}
				C%	N%	H%	
Ligand	Cream	108-112	54.12	72.1(71.53)	6.6(6.42)	7.5(7.39)	0.74
Hg LCl_2	Orange	133-135	68.27	43.9(44.10)	4.1(3.96)	4.6(4.56)	1.62
Hg LBr_2	Cream	150-153	92.21	40.1(39.18)	3.3(3.52)	4.1(4.05)	0.83
Hg LI_2	Cream	148-152	62.335	35.3(35.05)	3.3(3.14)	3.7(3.62)	1.33
Hg$L(N_3)_2$	Cream	108-113	87.91	43.1(43.30)	15.7(15.54)	4.6(4.47)	1.83
Hg$L(SCN)_2$	Cream	188-192	30.85	44.5(44.64)	7.3(7.44)	4.4(4.28)	7.35
Hg$L(NO_3)_2$	Yellow	154-157	28.62	41.2(41.03)	7.5(7.36)	4.4(4.24)	25.7

Table 2. Infra-red spectra (cm^{-1}) of the N_2O_2-Schiff base ligand (L) and its mercury complexes after drying at 150 ° C.

Compounds	νC-H alkene	νC-H aliph.	νC-H imine	ν(SCN/N_3/ NO_3)	ν (C=N)	ν(C=C)	ν(C-N)	ν(M-O)	ν(M-N)	λ(nm)
Ligand	3080	2955	2853	-	1633	1459 1443	1162	-	-	296
HgLCl_2	3004	2914	2869	-	1626	1441 1386	1168	571	535	314
HgLBr_2	3034	2927	2860	-	1625	1441 1426	1169	576	534	313
HgLI_2	3037	2922	2856	-	1624	1439 1424	1168	574	528	312
Hg$L(N_3)_2$	3034	2906	2855	2042	1633	1458 1439	1163	553	534	298
Hg$L(SCN)_2$	3031	2904	2866	2110, 2056	1635	1457 1439	1174	561	532	275, 318
Hg$L(NO_3)_2$	3066	2929	2869	1383 1510	1624	1459 1439	1169	608	528	313

Table 3. ^{1}H NMR spectral data of the N_2O_2-Schiff base ligand (L) and Hg(II) complexes in DMSO-d_6.

Compound	^{1}H NMR data (δ, ppm)
Ligand	7.99 (d, 2$H_{dd'}$, J = 8.7Hz), 7.52(d, 4$H_{gg'}$, J=8.7Hz), 6.99(d, 2$H_{ff'}$, J=15.7 Hz), 6.95(d, 2$H_{hh'}$, J =8.7 Hz), 6.76 (dd, 2$H_{ee'}$, J_1 = 16.0Hz , J_2 = 8.7Hz), 3.77 (s, 6$H_{ii'}$), 3.60 (m, 4$H_{bb'}$), 3.57 (m, 4$H_{cc'}$), 3.52 (s, 4$H_{aa'}$)
Hg LCl_2	8.26 (d, 2$H_{dd'}$, J = 8.3Hz), 7.60(d, 4$H_{gg'}$, J=8.3Hz), 7.30(d, 2$H_{ff'}$, J=15.4 Hz), 7.29 (dd, 2$H_{ee'}$, J_1 = 15.8Hz , J_2 = 7.4Hz), 6.98(d, 4$H_{hh'}$, J =8.5 Hz), 3.80 (s, 6$H_{ii'}$), 3.72 (m, 8$H_{bb'cc'}$), 3.60 (bs, 4$H_{aa'}$)
Hg LBr_2	8.23 (d, 2$H_{dd'}$, J = 8.7Hz), 7.59(d, 4$H_{gg'}$, J=8.7Hz), 7.21(m, 2$H_{ff'}$), 7.02 (dd, 2$H_{ee'}$, J_1 = 16.6Hz , J_2 = 8.4Hz), 6.97(d, 2$H_{hh'}$), 3.80 (s, 6$H_{ii'}$), 3.69 (bs, 8$H_{bb'cc'}$), 3.52 (s, 4$H_{aa'}$)
Hg LI_2	8.21 (d, 2$H_{dd'}$, J = 8.1Hz), 7.58(d, 4$H_{gg'}$, J=8.6Hz), 7.18(m, 4$H_{ff'ee'}$), 6.97(d, 4$H_{hh'}$, J=8.5Hz), 3.79 (s, 6$H_{ii'}$), 3.67 (bs, 8$H_{bb'cc'}$), 3.53 (bs, 4$H_{aa'}$)
Hg$L(N_3)_2$	8.02 (d, 2$H_{dd'}$, J = 8.7Hz), 7.54(d, 4$H_{gg'}$, J=8.7Hz), 7.02(d, 2$H_{ff'}$, J=16.2 Hz), 6.96(d, 4$H_{hh'}$, J =8.7 Hz), 6.78 (dd, 2$H_{ee'}$, J_1 = 16.0Hz , J_2 = 8.7Hz), 3.79 (s, 6$H_{ii'}$), 3.60 (bs, 8$H_{bb'cc'}$), 3.52 (s, 4$H_{aa'}$)
Hg$L(SCN)_2$	8.24 (d, 2$H_{dd'}$, J = 8.7Hz), 7.66(d, 4$H_{gg'}$, J=7.3Hz), 6.99(m,8$H_{hh',ff',ee'}$), 3.79 (s, 6$H_{ii'}$), 3.68 (bs, 8$H_{bb'cc'}$), 3.63 (s, 4$H_{aa'}$)
Hg$L(NO_3)_2$	8.26 (d, 2$H_{dd'}$, J = 8.1Hz), 7.89(d, 4$H_{gg'}$, J=8.9Hz), 7.15(d, 4$H_{hh'}$, J =8.7 Hz), 7.05 (d, 2$H_{ff'}$, J=15.8 Hz), 6.75 (dd, 2$H_{ee'}$, J_1 = 15.8Hz , J_2 = 7.8Hz), 3.84 (s, 6$H_{ii'}$), 3.70 (s, 8$H_{bb'cc'}$), 3.64 (s, 4$H_{aa'}$)

Table 4. ^{13}C NMR spectral data of the Schiff base ligand (L) and mercury complexes in DMSO-d_6.

Compound	^{13}C NMR data (δ, ppm)
Ligand	164.31($C_{4,4'}$), 160.53($C_{10,10'}$), 141.55($C_{6,6'}$), 129.23 ($C_{7,7'}$), 128.63($C_{8,8'}$), 126.28 ($C_{9,9'}$), 114.75 ($C_{5,5'}$), 70.74 ($C_{2,2'}$), 70.14 ($C_{1,1'}$), 60.72 ($C_{11,11'}$), 55.66 ($C_{3,3'}$)
Hg LCl_2	168.64($C_{4,4'}$), 161.33($C_{10,10'}$), 145.89($C_{6,6'}$), 129.96 ($C_{7,7'}$), 128.20($C_{8,8'}$), 124.21 ($C_{9,9'}$), 114.97 ($C_{5,5'}$), 70.29 ($C_{2,2'}$), 69.82 ($C_{1,1'}$), 60.32 ($C_{11,11'}$), 55.82 ($C_{3,3'}$)
Hg LBr_2	167.83($C_{4,4'}$), 161.22($C_{10,10'}$), 145.21($C_{6,6'}$), 129.84 ($C_{7,7'}$), 128.27($C_{8,8'}$), 124.49 ($C_{9,9'}$), 114.95 ($C_{5,5'}$), 70.27 ($C_{2,2'}$), 70.07 ($C_{1,1'}$), 60.38 ($C_{11,11'}$), 55.80 ($C_{3,3'}$)
Hg LI_2	167.16($C_{4,4'}$), 161.10($C_{10,10'}$), 144.51($C_{6,6'}$), 129.72 ($C_{7,7'}$), 128.75($C_{8,8'}$), 124.83 ($C_{9,9'}$), 114.92 ($C_{5,5'}$), 70.22 ($C_{2,2'}$), 70.17 ($C_{1,1'}$), 60.25 ($C_{11,11'}$), 55.83 ($C_{3,3'}$)

$HgL(N3)_2$	164.34($C_{4,4'}$), 160.54($C_{10,10'}$), 141.60($C_{6,6'}$), 129.26 ($C_{7,7'}$), 128.71($C_{8,8'}$), 126.31 ($C_{9,9'}$), 114.77 ($C_{5,5'}$), 70.75 ($C_{2,2'}$), 70.15 ($C_{1,1'}$), 60.75 ($C_{11,11'}$), 55.69 ($C_{3,3'}$)
$HgL(SCN)_2$	164.82($C_{4,4'}$), 161.61($C_{10,10'}$), 144.84($C_{6,6'}$), 129.93($C_{7,7'}$), 129.26($C_{8,8'}$), 126.60 ($C_{9,9'}$), 114.46 ($C_{5,5'}$), 70.72 ($C_{2,2'}$), 70.06 ($C_{1,1'}$), 60.59 ($C_{11,11'}$), 56.53 ($C_{3,3'}$)
$HgL(NO_3)_2$	164.71($C_{4,4'}$), 162.26($C_{10,10'}$), 153.76($C_{6,6'}$), 132.30($C_{7,7'}$), 131.21($C_{8,8'}$), 130.13 ($C_{9,9'}$), 115.0 ($C_{5,5'}$), 70.11 ($C_{2,2'}$), 70.04 ($C_{1,1'}$), 60.10 ($C_{11,11'}$), 56.17 ($C_{3,3'}$)

2.4. Biological study (In vitro)

The biological activities of the synthesized compounds were evaluated by the well diffusion method. For this purpose, bacterial strains including *Escherichia coli and Pseudomonas aeruginosa* (as Gram-negative bacteria); *Staphylococcus and Bacillus Subtilis* (as Gram-positive bacteria) and two fungal species such as *Aspergillus oryzae* and *Candida albicans* were studied. To evaluate the antibacterial properties, initially, three different concentrations of the test compounds were made in DMSO solvent. The selected bacteria were added to the tubes containing Müller Hilton Broth liquid culture medium and then the test tubes were kept in an incubator for 24 h at 37°C to prepare an enriched culture. Then, the Müller-Hinton agar medium was prepared according to the manufacturer's instructions, and 100µL of the Müller-Hinton broth culture medium containing the selected bacteria was poured onto the agar medium using a micropipette and spread evenly with a sterile swab. The test samples including ligand and complexes with concentrations of 10, 20 and 40 mg/ml (dissolved in DMSO as a solvent) were prepared and then 50µl of the trial test samples were poured into wells made on prepared plates with a diameter of 6 mm and then incubated for 24h at 37°C. After incubation time, the diameter of the inhibited bacterial/fungal growth zone around each well was measured as antimicrobial activity of the test samples.

2.5. Investigation of minimum inhibitory concentration (MIC) and minimum bactericidal concentration (MBC)

The minimum concentration required to prevent the growth of bacteria after 24 hours of incubation at 37°C is defined as MIC and was measured based on the serial dilution method. The minimum concentration that microorganisms do not grow in the fresh culture medium is named as the MBC and was performed by seeding a complete loop (0.001 ml) of culture medium containing the test sample prepared on the plates containing culture medium of Müller Hilton agar, and then it was kept in an incubator for 24 hours at 37°C.

2.6. DNA cleavage potential

The DNA cleavage ability of the synthesized compounds was investigated by using the DNA of Escherichia coli by agarose gel electrophoresis technique. The extraction of DNA was performed according to our previous report [40]. Samples were prepared at the concentration of 5 mg/ml in DMSO as solvent. In separate micro-tubes, 4 µl of the prepared samples were added to the 4µl of extracted DNA and then incubated for 2h at 37°C. Also, extracted pure DNA and DNA treated with 30% H_2O_2 were used as the negative and positive controls, respectively. Then the sample containing DNA was mixed with bromophenol blue dye. Finally, the mixture of DNA and test compound along with the positive control, negative control and the ladder were loaded into the wells, and electrophoresis was performed at 100 volts constant for 30 min. The obtained bands due to DNA cleavage were observed by UV light and then photographed.

2.7. Cell culture of the PC3 (prostate cancer) cell lines

Cells in a complete culture medium containing 90% DMEM/F12, 10% fetal bovine serum (FBS), and 1% antibiotic (penicillin / Streptomycin) were cultured in a flask (25 mL) and then were kept in an incubator at 90% humidity and 5% CO_2 atmosphere for 24 h and 37°C. When the cells reached the desired morphology, they were used to perform the designed tests.

2.8. Cytotoxicity test

2.8.1. 3-(4,5-dimethylthiazol-2-yl) -2,5- diphenyl tetrazolium (MTT) method

Cytotoxicity of the compounds was evaluated by MTT method. MTT test is a color evaluation method based on the enzymatic reduction of yellow solution of 3-(4,5-dimethylthiazol-2-yl)-2,5-diphenyltetrazolium bromide (MTT) and the formation of water-insoluble purple crystals, formazan (scheme 2) [41]. PC3 cells at a density of 10^4 cells per well were seeded in 96-well plates at 37°C, 5% CO_2 and after 24 h of incubation were treated with concentrations of 10, 20, 30, 40 and 50µg/ml of the test compounds for 24 h. At the end of 24 h of treatment, 10µl of MTT solution (5mg/ml) was added to each well and the 96-well plates were kept in an incubator at 37°C for 4 h. Finally, the absorption of the formed formazan was recorded at 570 nm by an ELISA reader device (800TS. Microplate reader).

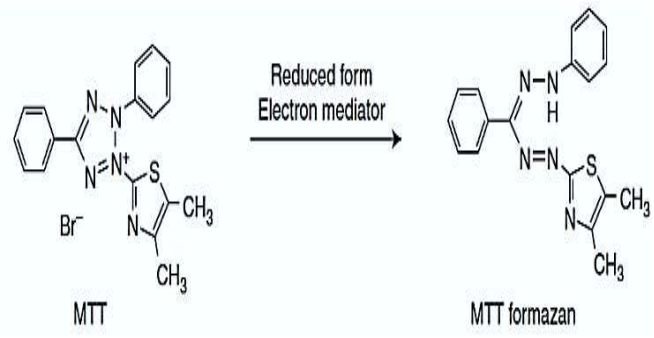

Scheme 2. Reduction of MTT to MTT formazan.

2.8.2. Evaluation of nitric oxide level

Nitric oxide, which is produced by the activity of the enzyme nitric oxide synthase, is an unstable compound and is rapidly converted to nitrate and nitrite. Therefore, nitrate/nitrite concentration is an indicator of nitric oxide production, measured by the Griess method [42]. In this method, Griess reagent (1% sulfanilamide, 0.1% N-(1-naphthyl)ethylene diamine dihydrochloride in 2.5% phosphoric acid) is added to the test sample to measure nitrate concentration. Therefore, PC3 cells were removed from the incubator after 24 h of treatment with effective drug concentrations, and the supernatant of the culture medium was transferred from the culture plates to vials (1.5 ml). After centrifugation for 7 min., 100µl of each test sample was transferred to the well of 96-well plates. Then about 100 µl of Griess reagent was added to each well and placed in the dark for 10 min. at ambient temperature. Finally, the absorbances were read by the ELISA reader at 570 nm.

2.10. Investigation of antioxidant activity

The antioxidant activities of the compounds were investigated by 1, 1-diphenyl-2-picryl-hydrazyl (DPPH) and Ferric Reducing Antioxidant Power (FRAP) assays. DPPH assay is a standard and rapid technique for studies of antioxidant activity and also for the assessment of the free radical scavenging effects of the compounds [43] and the FRAP method is based on reducing the colorless Fe^{3+}-TPTZ complex into the Fe^{2+}-TPTZ (intense blue) complex when interacting with an antioxidant [44].

2.10.1. DPPH assay

In the DPPH assay, the antioxidant activities of the ligand and Hg(II) complexes were measured by the degree of decolonization of the DPPH solution. For this purpose, different concentrations (25 to 400 µg/mL) of the test compounds were prepared. 100 µl of the prepared concentrations of the test samples was added to 1 ml of the methanolic solution of DPPH (1 mM), and then the reaction mixture was shaken and placed in the dark for 15min. and the absorbance was measured at 517 nm by the spectrophotometer. To compare the antioxidant activity of the test compounds, ascorbic acid was used as a standard antioxidant. The inhibition abilities of the free radicals were obtained using the following equation (Eq.1) and the results have been reported as IC_{50}.

Eq. 1:

DPPH scavenging percent (%)= $[(A_0 - A_s)/A_0] \times 10$

A_0 is absorbance of the control and A_s is absorbance of the test compound. Furthermore, ascorbic acid equivalent antioxidant capacities (AEAC) for the ligand and mercury complexes were calculated by equation 2 (Eq. 2).

Eq. 2:

AEAC (mg AA/ g dry weight (test sample))= (IC_{50} ascorbic acid/IC_{50} Sample)× 100

2.10.2. FRAP Assay

FRAP reagents included $FeCl_3$ (2 mM) in acetate buffer (300 mM, pH=3.6) and TPTZ (2, 4, 6-tripyridyl-s-triazine)(10 mM) in HCl (40 mM). The working FRAP reagent was prepared using a mixture of 50 ml of acetate buffer, 5ml of $FeCl_3$, and 5ml of TPTZ in a ratio of 10:1:1. Also $FeSO_4.7H_2O$ (2 mM) in methanol was used as standard. To FRAP assay, 5 mg of each test sample was dissolved in 100 µl of DMSO and 900 µl of water was added to it. Then, 1000 µl of working FRAP reagent was added to 50 µl of each test sample and stirred for a few minutes. After 15 min. the adsorption was read at 595 nm.

3. Results and discussion

3.1. Physical and analytical data

The ligand and its mercury complexes were obtained as colored powders that were stable at room temperature. The mercury complexes were obtained by addition of the tetradentate N_2O_2 ligand to an ethanolic solution of mercury salts (HgX_2; X=Cl^-, Br^-, I^-, N_3^-, NO_3^- and SCN^-). For mercury complexes, the general formula $HgLX_2$ is suggested, which indicates a 1:1 ratio between the ligand and the mercury salt. The synthesized compounds are insoluble in water and alcohols such as ethanol and methanol but are soluble in some organic solvents such as DMF and DMSO. The melting point of the ligand is in the range of 108-112°C meanwhile the mercury complexes are decomposed at about 108-192 °C. These coordination compounds are stable solid at

ambient temperature but are decomposed at high temperatures.

The molar conductivities of the ligand and its Hg(II) complexes were measured in DMF solution (2×10^{-5}M) that were found in the range of 0.74- 25.70 $cm^2 \Omega^{-1}mol^{-1}$ at ambient temperature so it can be concluded that halide/pseudohalide ions and N_2O_2-tetradentate Schiff base ligand have been bound to the metal center meaning the mercury complexes are non-electrolyte at room temperature [45-49]. According to the conductivity values of the complexes, it was found that the $HgL(NO_3)_2$ complex is the most unstable compound with the highest ionic dissolution in solution and the $HgLBr_2$ complex has the highest stability in solution with the lowest dissolution in the solvent.

3.2. FT/IR spectra

The IR spectra of the synthesized compounds were recorded as KBr disks in the range of 4000–400 cm^{-1}. In the IR spectrum of the ligand, the strong peak appeared at 1633cm^{-1} belongs to the iminic (C=N) group and the absence of adsorption bands at 1685 cm^{-1} related to the 4-methoxycinnamaldehyde (C=O group) and at 3260-3380 cm^{-1} related to the NH_2 group of 1,8-diamino-3,6-dioxaoctane confirm the formation of the Schiff base ligand [50, 51].

Aromatic and aliphatic C-H stretching vibrations appeared at 2955 cm^{-1} and 3080 cm^{-1}, respectively. A peak at 2853 cm^{-1} region is related to iminic C-H that changes after coordination. The IR spectra of the synthesized complexes are similar to the IR spectrum of the free ligand but the position or intensity of the absorption bands may change as compared with the free ligand. In the mercury complexes, the absorption band at 1624-1635 cm^{-1} belongs to the iminic (C=N) group shifting about 2 to 9 cm^{-1} to the lower or higher frequencies with respect to the ligand spectrum proving the coordination of the ligand to the mercury(II) center [52-54].

The main reason for these shifts may be related to the π-back bonding of d^{10}-orbital of metal to π* of azomethine bond of ligand [55]. The presence of weak absorption peaks in the range of 500-570 and 600-640 cm^{-1} confirm the formation of M-O and M-N bonds respectively. In the IR spectrum of $HgL(SCN)_2$, two peaks appearing at 2110 and 2055 cm^{-1} belongs to the coordinated SCN^-. In the IR spectrum of $HgL(N_3)_2$, a stretching vibration appeared at 2042 cm^{-1} indicates the presence of the coordinated azide group. For instance, Fig. 1 illustrates the FT/IR spectra of the ligand and mercury complexes.

The UV-visible electronic spectrum of the free ligand displays an absorption band at 296 nm assigned to $\pi \rightarrow \pi^*$ electronic transition of aromatic and azomethine π-systems shifts to longer wavelengths in the range of 298-318 nm in the synthesized complexes that confirms coordination of the ligand [52, 54, 56]. The UV-visible spectra of all compounds are illustrated in Fig. 2.

3.4. ^1H and ^{13}C NMR spectra

For more confirmation of synthesis of the compounds, ^1H and ^{13}C NMR spectra of the ligand and its mercury complexes were recorded and the chemical shift data (δ, ppm) as well as full assignments of them based on the suggested structure (scheme 1) have been collected in

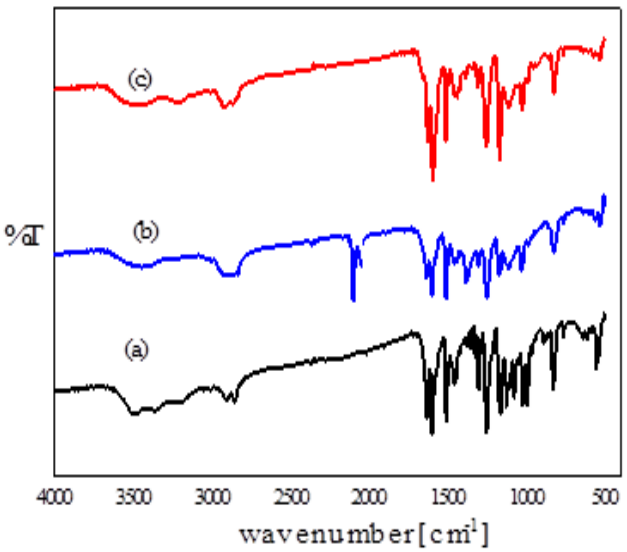

Fig. 1. FT/IR spectra: (a) ligand, (b) $HgL(SCN)_2$, and (c) $HgLCl_2$ complexes (after drying at 150 ° C).

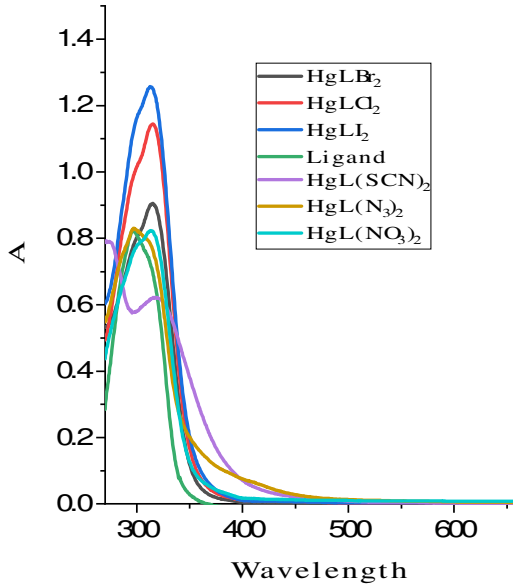

Fig. 2. UV-visible spectra of the free ligand and its Hg(II) complexes.

tables of 3 and 4. Also as typical spectra, the ^{1}H NMR spectra of the ligand and its mercury azide complex have been presented in Fig. 3.

In the ligand spectrum, signals at 7.99 ppm, (7.52 and 6.99 ppm), (6.95 and 6.76 ppm), (6.99 and 6.76) and 3.77-3.52 ppm with related coupling constant as found in Table 3 are assigned to azomethin(iminic), aromatic, olefinic and aliphatic hydrogens respectively that are well in agreement with the suggested structure.

After coordination of the ligand to mercury (II) ion, these signals are up or downfielded to new chemical shifts into the ranges of (8.02-8.26 ppm), (7.54-7.89, 6.96-7.15ppm), (7.02-7.30, 6.75-7.29 ppm) and (3.84-3.52 ppm) respectively confirming the successful synthesis of mercury(II) complexes. Furthermore, the carbon NMR signals at 164.31 ppm, (160.53 and 126.28 ppm), (141.55 and 114.75 ppm) and (70.74-55.66 ppm) are attributed to iminic, aromatic, olefinic and aliphatic carbons of the free ligand. The iminic carbon signal as characteristic one is downfielded to 168.84-164.3 ppm after complex formation confirming binding of the ligand to mercury center via imine nitrogen well.

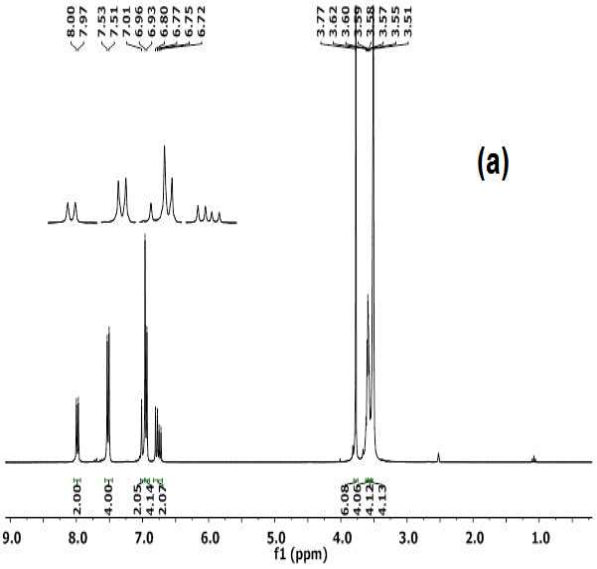

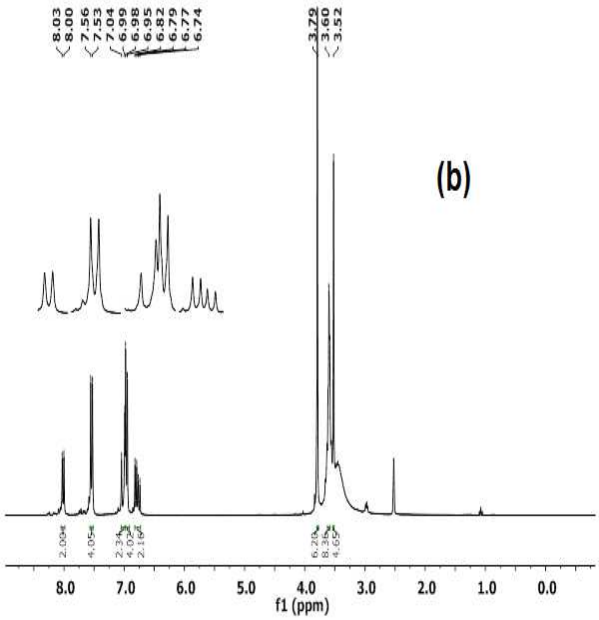

Fig. 3. The ^{1}H NMR of the ligand (a) and $HgL(N_3)_2$ (b).

Other assigned carbon signals as collected in Table 4 are as another spectral evidences for the suggested structure of the mercury complexes as shown in scheme 1.

3.5. ESI/Mass spectra

The mass spectra of the complexes were recorded by ESI/Mass technique applying ionization method. As typically, Fig. 4 depicts mass spectra of the ligand and $HgLBr_2$ complexes. According to the mass spectral data, the presence of a peak at m/z value of 437 confirms suggested structure of the ligand with molecular weight of 436 g/mol. The m/z peak values in the mass spectra at 799 and 797 well confirm formation of the $HgLBr_2$ complex. Also, appearance of the peaks at m/z values of 708, 891, and 753 in related mass spectra indicate successfully synthesis of the $HgLCl_2$, $HgLI_2$ and $HgL(SCN)_2$ complexes, respectively (Fig.4).

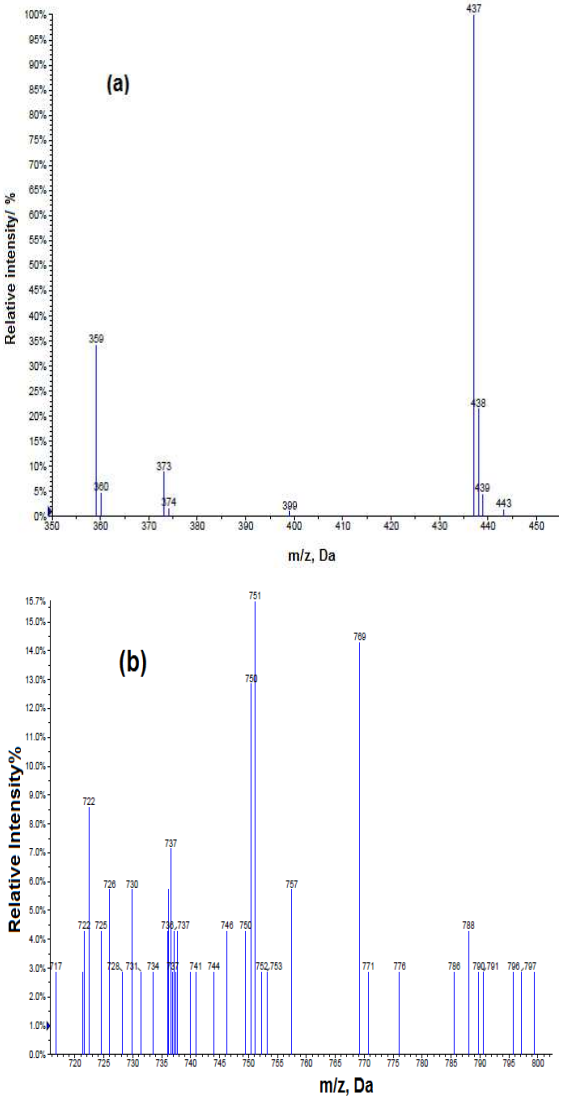

Fig.4. The mass spectra of a) Ligand, b) $HgLBr_2$.

3.6. Investigation of thermal behavior

The thermal stabilities of the ligand and its mercury complexes were investigated in the temperature range of 25 to 1000°C at a heating rate of 20 °C/min. under nitrogen atmosphere. For example, the thermal plots (TG/DTG/DTA) of the free ligand and mercury chloride complex are given in Fig. 5 meanwhile the rest of the thermal plots of the others are found in supplementary file as fig. 1S. Thermal analysis data such as thermal decomposition steps, reduced mass percentage in each step (mass loss experimentally and theoretically), the proposed departed fragments, the final residual component and thermo-kinetic activation parameters have been reported in tables of 5 and 6. Thermal decomposition of the ligand occurs in the temperature range of 25 to 800°C via three steps.

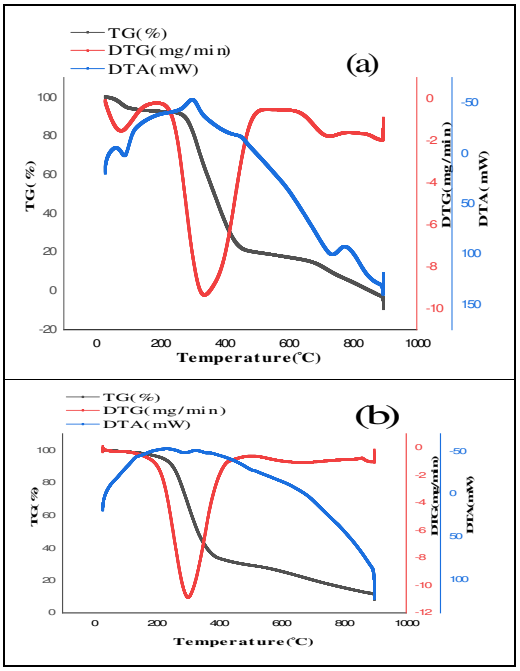

Fig.5. TG/DTG/DTA plots of (a) Schiff base ligand, (b) $HgLCl_2$ complex.

The reduced mass equal to 7.3 % at first step at temperatures below 200°C is related to crystalline/hydrated water (1.87 H_2O) in the ligand structure. The reduced weight at the second step in the temperature range of 195-580°C suggests the departure of the $C_{24}H_{26}N_2O_2$ fragment. The thermal decomposition of the ligand at the third step (580-790°C) accompanied with a mass loss of about 12.58 % (Calculated, 13.18 %), which may be attributed to the elimination of the $C_2H_6O_2$ segment. The thermal decomposition diagrams of the $HgL(SCN)_2$ and $HgL(N_3)_2$ complexes (Fig. 1S) show mass loss percentages (about 3.4 and 5.8 % respectively) under 200°C confirming the presence of crystalline or hydrated water molecules (equal to 1.47 and 2.46 H_2O respectively) in their structures. In addition to the water elimination step, three steps of thermal decomposition have been observed for the $HgL(SCN)_2$ complex and two steps for the $HgL(N_3)_2$ complex respectively with suggested segments in the table 5. $HgLCl_2$, $HgLI_2$, $HgLBr_2$ and $HgL(NO_3)_2$ complexes are decomposed via two consecutive steps while in the thermal decomposition diagrams of these complexes, no weight loss was observed in the temperature range of 25 to 200 °C indicating absence of crystalline or hydrated water in their structure. At the end, $HgLX_2$ (X= I^- and NO_3^-) complexes left out some amounts of unknown mercury salt as residual. Moreover, thermo-kinetic activation parameters of the ligand and all mercury complexes for all decomposition steps including activation energy (ΔE^*), enthalpy of activation (ΔH^*), entropy Change (ΔS^*), Gibbs free energy change (ΔG^*), and Arrhenius constant (A) at each step, were evaluated using the Coats – Redfern

equation [58]. The lowest value of activation energy (17.721 kJ/mol) is related to the first step of $HgL(N_3)_2$ thermal decomposition, while the highest value of activation energy is found for the first step of $HgL(SCN)_2$ thermal decomposition (76.458 kJ/mol). Positive values of ΔH^* (12.943 to 72.032 kJ/mol) indicate that all thermal decomposition steps are endothermic. Negative ΔS^* values show that the reaction rate of these compounds is slower than normal decomposition reactions and on the other hand more ordered activated complex than the reactants are formed during the decomposition processes [59]. Finally, the positive values of ΔG^* in the range of (1.88 to 4.22) $\times 10^2$ kJ/mol, reflect non-spontaneous nature of all thermal decomposition steps [60].

3.7. Antimicrobial activity (In vitro)

The biological activities of the synthesized compounds were evaluated against four types of bacteria including *S. aureus* and *B. subtilis* as Gram-positive bacteria and *Escherichia coli* and *Pseudomonas aeruginosa* as Gram-negative bacteria by well diffusion method. The antibacterial data from the study of antimicrobial screening as the zone diameter of inhibition from the growth (mm) have been summarized in Table 7. A comparative evaluation of the obtained results revealed that the coordination of the ligand to mercury ion increases the antibacterial activity with respect to the free ligand. According to the results in Table 7, $HgLI_2$ complex shows the highest inhibitory against P. *aeruginosa* with an inhibition zone diameter of 46.9 mm, *S. aureus* (40.64 mm), and B. *subtilis* (35 mm). The highest effect against E. *coli* is related to the $HgLBr_2$ complex whereas the ligand shows the weakest bactericidal against all the above mentioned bacteria. It should be noted that the comparison of the obtained results with standard drugs (*amoxicillin, penicillin, and cephalexin*) [61] showed the acceptable activities for the synthesized compounds against all the selected bacteria. For more clearance, Fig. 6 shows antibacterial activity of the ligand and its mercury complexes in terms of zone diameter of inhibition from the growth (mm) as bar graphs. In addition to the above studies, MIC and MBC tests were performed for all mercury complexes using the serial dilution method and the data have been tabulated as Table 8. In MIC and MBC tests, lower values indicate better antimicrobial activity. Against B. *subtilis*, the $HgLI_2$ and $HgL(SCN)_2$ complexes have been shown the best growth inhibitory effects as compared to other compounds and the least inhibitory effect was related to a ligand. About the *S. aureus*, $HgLI_2$, $HgLCl_2$ and $HgL(N_3)_2$ complexes had the lowest MIC(39.06 µg/mL) and the highest MIC(1250µg/mL) for this bacterium was belonged to the ligand and $HgL(NO_3)_2$. Among the tested compounds, $HgLI_2$ and $HgLCl_2$ with the same MIC value of 19.53µg/mL, demonstrated the same activity against *P. aureus* meanwhile the lowest antibacterial activity was observed for the ligand. Finally, $HgL(NO_3)_2$ complex showed the lowest amount of MIC(156.25µg/mL)

Table 5. Thermal analysis data for the Schiff base ligand and its mercury complexes (dried at room temperature) including temperature range, mass loss%, differential thermal gravimetric (DTG) peak, proposed segments and final residuals.

Compound	Temperature range/˚C	Mass loss [found (calculated)]/ %	DTG peak/˚C	Proposed segment	Final residue
Ligand. 1.87 H_2O	25-110	7.30	100.5	1.87 H_2O	-
	195-580	78.85 (79.46)	349.59	$C_{24}H_{26}N_2O_2$	
	580-790	12.58 (13.18)	729.5	$C_2H_6O_2$	
Hg LCl_2	120-496	70.54 (71.246)	303.07	$C_{26}H_{32}Cl_2N_2O_4$	-
	496-745	11.43 (10.817)	686.38	$Hg_{0.96}$	
Hg LBr_2	177-484	65.74 (65.363)	321.44	$C_{26}H_{32}BrN_2O_4$	-
	484-703	33.68 (33.138)	635.52	$Hg_{0.98}Br$	
Hg LI_2	120-440	54.64 (48.998)	331.62	$C_{26}H_{32}N_2O_4$	Unknown mercury salt
	440-600	20.40 (21.38)	458.68	$I_{1.5}$	
$HgL(N_3)_2$. 2.46 H_2O	25-120	5.8	100.4	2.46 H_2O	-
	106-421	62.70 (63.23)	259.5	$C_{26}H_{32}N_5O_4$	
	421-709	31.53(32.053)	541.86	HgN_3	
$HgL(SCN)_2$. 1.47 H_2O	25-120	3.4	100.2	1.47 H_2O	-
	184-362	39.28 (38.09)	259.2	$C_{20}H_{22}O_2$	
	362-540	18.73 (18.01)	377.94	$C_6H_{10}N_2O_2$	
	540-885	38.63 (38.39)	824.93	$C_2N_2S_{1.5}Hg_{0.97}$	
$HgL(NO_3)_2$	200-360	44.05 (43.67)	266.9	$C_{21}H_{22}N_2O_2$	Unknown mercury salt
	360-640	39.46 (40.329)	485.86	$C_4H_{10}N_2O_7Hg_{0.4}$	

Table 6. Thermo-kinetic activation parameters of the thermal decomposition steps of the Schiff base and mercury complexes.

Compound	Decompositionstep(˚C)	E^*(kJmol^{-1})	A^*(s^{-1})	ΔS^*(kJmol^{-1}K^{-1})	ΔH^*(kJmol^{-1})	ΔG^*(kJmol^{-1})

Ligand	195-580	41.51	4.22×10^{-1}	-3.22×10^{2}	36.33	2.37×10^{2}
	580-790	38.82	1.27×10^{-2}	-3.55×10^{2}	30.48	3.86×10^{2}
Hg LCl_2	120-496	56.63	7.87×10^{1}	-2.78×10^{2}	51.84	2.12×10^{2}
	496-745	25.61	2.47×10^{-3}	-3.68×10^{2}	17.63	3.71×10^{2}
Hg LBr_2	177-484	51.77	2.99×10^{1}	-2.86×10^{2}	46.83	2.17×10^{2}
	484-703	37.77	1.61×10^{-2}	-3.52×10^{2}	30.24	3.49×10^{2}
Hg LI_2	120-440	47.99	4.39	-3.02×10^{2}	42.96	2.26×10^{2}
	440-600	19.25	1.29×10^{-3}	-3.71×10^{2}	12.94	2.95×10^{2}
$HgL(N_3)_2$	106-421	17.72	2.60×10^{-3}	-3.63×10^{2}	13.29	2.06×10^{2}
	421-709	35.33	2.21×10^{-2}	-3.48×10^{2}	28.56	3.13×10^{2}
$HgL(SCN)_2$	184-362	76.46	9.33×10^{4}	-2.18×10^{2}	72.03	1.88×10^{2}
	362-540	22.73	4.97×10^{-3}	-3.59×10^{2}	17.31	2.51×10^{2}
	540-885	52.87	4.54×10^{-2}	-3.45×10^{2}	43.74	4.22×10^{2}
$HgL(NO_3)_2$	200-360	74.05	4.23×10^{4}	-2.25×10^{2}	69.56	1.91×10^{2}
	360-540	50.58	5.21	-2.39×10^{2}	44.29	2.25×10^{2}

against *E. coli*. The various mechanisms may be effective on the bactericidal activity of the compounds. Therefore suggestion an accurate mechanism for the bactericidal function is not possible. Two important pathways are destruction of the cell membrane via diffusion through it and destructive effects on the DNA of the bacteria after diffusion into the microbe cells. Both two agents can effectively lead to death of the bacteria. Regarding the results on DNA cleavage potency of the compounds, it is suggested that the less polar complexes can diffuse into cells better than more polar complexes and therefore may lead to bactericidal by DNA cleavage after effective diffusion. On the other hand more polar complexes involve the coordination with the donor atoms of membrane cell structures leading to rupture of membrane, evacuating the cytoplasm and finally death of microorganism. In current study, it is suggested that the mercury iodide, bromide, chloride and thiocyanate complexes are less polar with respect to mercury azide and nitrate as more polar complexes and may act as bactericidal compounds based on previous explanation. In the next section, about the DNA cleavage potential of the compounds will be discussed but herein about the cell membrane destruction by some typical compounds as compared with parent ligand is briefly pointed out. Accordingly, scanning electron microscopic images (SEM) were used to confirm the destructive effect of ligand and mercury complexes against selected bacteria. For example, the destructive effect of $HgLCl_2$ complex and free ligand against *B. subtilis* and the destructive effect of $HgLI_2$ complex and ligand against *E. coli* were depicted in fig. 7. According to the above mentioned results, $HgLCl_2$ and $HgLI_2$ showed more destructive (antimicrobial) effect than free ligand so that the SEM images show more cellular degradation of *E. coli* and *B. subtilis* by the complexes than free ligand respectively.

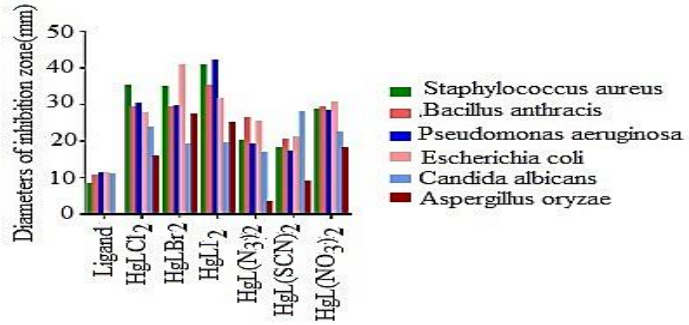

Fig. 6. Antibacterial activities of ligand and its mercury complexes as zone of inhibition from the growth(mm) for the compound concentration of 40 mg/mL.

In fact, the effect of both compounds on these bacteria is observed to be compaction, elongation of cell length, blistering, hole formation in the cell wall and eventually, rupture of the cytoplasmic membrane and

leak of cell membrane contents. However, in the case of ligand, these changes were less observable against both bacteria.

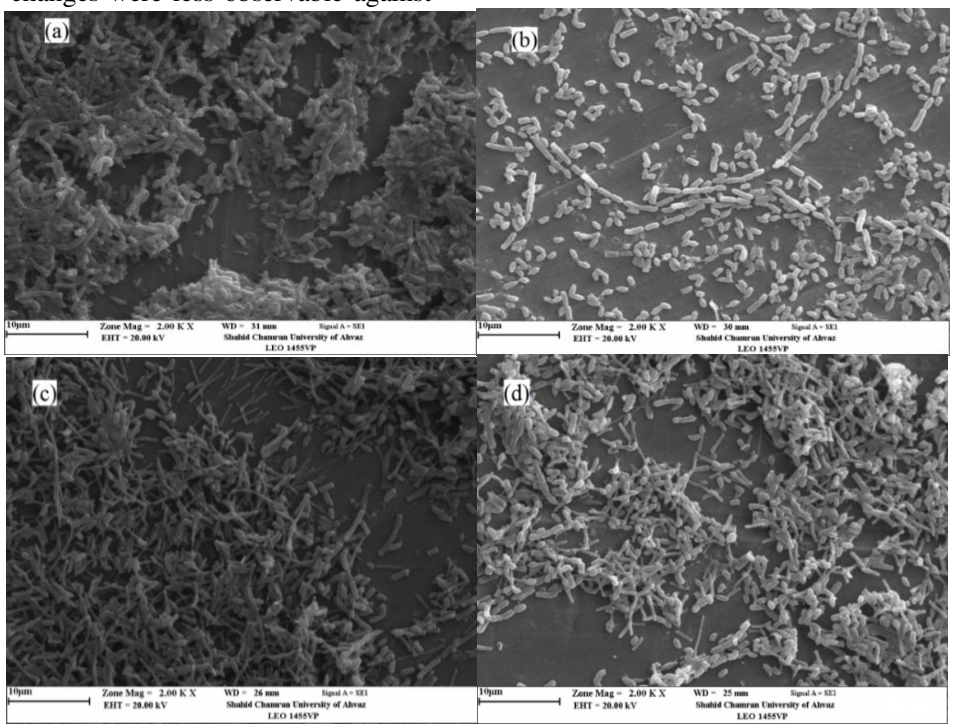

Fig. 7. The SEM images after treatment of *B. subtilis* by (a) $HgLCl_2$ and (b) ligand, *E. coli* by (c) $HgLI_2$ and (d) ligand.

Table 7. Antibacterial activities of the free ligand and mercury (II) Compounds as diameter of the growth inhibition zone (mm) around constructed wells against bacteria.

Compound	Gram-positive						Gram-negative					
	S. aureus			*B. subtilis*			*P. aeruginosa*			*E. coli*		
	10	20	40	10	20	40	10	20	40	10	20	40
Ligand	-	6	8	-	8.4	10.4	6.0	8.2	11.0	-	6.4	11.2
$HgLCl_2$	25.7	31.9	35.1	19.5	23.2	29	17.9	29.7	30	23.5	25.0	27.5
$HgLBr_2$	21.6	30.1	34.6	23.0	27.0	29	21.2	27.2	29.5	24.6	30.7	40.6
$HgLI_2$	35.4	40.4	40.6	26.5	28.0	35	38.4	39.5	46.9	24.3	26.8	31.3
$HgL(N_3)_2$	12.5	15.5	20.0	19.5	23.2	26	16.2	17.6	19.0	17.5	22.4	25.0
$HgL(SCN)_2$	10.7	15.5	17.9	16.6	19.0	20.3	16.2	16.8	17.0	15.3	18.7	20.8
$HgL(NO_3)_2$	23.6	28.1	28.4	17.5	24.0	29	18.0	23.6	28.0	24.8	26.8	30.4
DMSO	-	-	-	-	-	-	-	-	-	-	-	-

Table 8. The values of the MIC and MBC data for the N_2O_2-Schiff base ligand and Hg(II) complexes for growth inhibition effect (μg/mL).

Compound	*S. aureus*		*B. subtilis*		*P. aeruginosa*		*E.coli*	
	MIC	MBC	MIC	MBC	MIC	MBC	MIC	MBC
Ligand	1250.0	2500.0	-	-	1250.0	5000.0	-	-

$HgLCl_2$	39.0	78.125	312.5	625.0	19.53	39.06	312.5	625
$HgLBr_2$	156.2	312.5	312.5	625.0	39.06	78.125	312.5	625
$HgLI_2$	39.0	78.125	156.25	312.5	19.53	39.06	312.5	625
$HgL(N_3)_2$	39.0	78.125	312.5	625	156.25	312.5	2500	5000
$HgL(SCN)_2$	78.125	156.25	156.25	312.5	156.25	312.5	5000	10000
$HgL(NO_3)_2$	1250	2500	312.5	625	78.125	156.25	156.25	312.5

3.8. Antifungal activity

A. oryzae and *C. albicans* were selected for antifungal activity test by the well diffusion method. The results have been reported based on the diameter of the inhibition zone from the growth (in mm) in Table 9. According to the results, in the case of *A. oryzae*, the highest inhibition effect was related to $HgLBr_2$ and the lowest effectiveness was found for $HgL(N_3)_2$. It is proposed the $HgLBr_2$ with relative lower polarity than others effectively diffuses into the microorganism cell and bind with DNA causing its cleavage and fungicidal activity. Also, against *C. Albicans*, $HgL(SCN)_2$ showed the best antifungal activity whereas ligand showed the lowest inhibitory effect. It is proposed that the $HgLBr_2$ and $HgL(SCN)_2$ with moderate polarity with respect to others effectively diffuses into the microorganism cell and bind with DNA causing its cleavage and fungicidal activity. It is obvious that the coordination capacity of the metal complexes for binding to cell membrane or DNA structure leading to cleavage is the main reason for superior activity of them with respect to free ligand.

Table 9. Antifungal activities of the ligand and its mercury complexes as diameter of inhibition zone (mm) around the well (filled with 40, 20, and 10 mg/mL) against two fungi.

Compound	***C. Albicans***			***A. oryzae***		
	10	20	40	10	20	40
Ligand	6.2	8.5	10.6	-	-	-
Hg LCl_2	17.1	20.2	23.6	11.9	13.6	15.5
Hg LBr_2	14.4	18.8	19.1	21.3	22.2	27.1
Hg LI_2	18.0	18.4	19.3	21.2	22.0	24.9
$HgL(N_3)_2$	7.6	9.4	16.5	-	-	3.2
$HgL(SCN)_2$	17.4	18.5	27.7	-	-	8.8
$HgL(NO_3)_2$	16.8	17.4	22.2	12.8	14.5	18.0

3.9. Investigation of the destructive interaction of the compounds with DNA

The ability of DNA cleavage of the synthesized compounds was investigated by agarose gel electrophoresis method using DNA extracted from *E. coli* and the image is shown in Fig.8. In this Fig, P, La and N bands are related to pure bacterial DNA (positive control agent), ladder and a mixture of H_2O_2 and DNA as negative control test respectively. Lane L is attributed to ligand and Lanes A to F are belonged to $HgLCl_2$, $HgLBr_2$, $HgLI_2$, $HgL(SCN)_2$, $HgL(NO_3)_2$ and $HgL(N_3)_2$ respectively. Having behavior similar to N can indicate the ability of the test compounds to cleave DNA meanwhile similar behavior with P confirms the lack of cleavage ability for the compound. According to fig.8, $[HgLI_2]$ complex showed the best destructive interaction with DNA. Then $[HgLBr_2]$ and $[HgL(SCN)_2]$ complexes had good destructive effects on DNA. Ultimately $[HgL(NO_3)_2]$, $[HgL(N_3)_2]$, ligand and $[HgLCl_2]$ compounds showed respectively lower destructive effect on DNA structure. It seems the more spherical and less polar complexes such as mercury halides and thiocyanate complexes can better diffuse between two strains of DNA causing the cleavage with respect to mercury azide and nitrate complexes that can strongly bind to outer coordinating donor atoms of DNA strains.

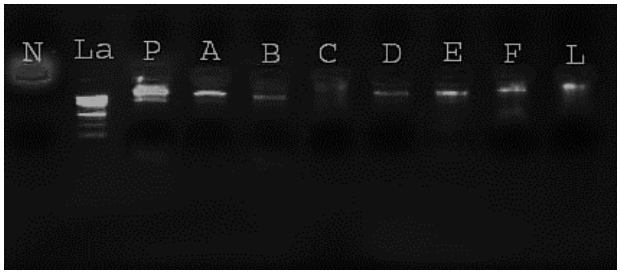

Fig.8. DNA cleavage potency of free N_2O_2-Schiff base ligand and its mercury complexes. Lanes: A: $HgLCl_2$, B: $HgLBr_2$, C: $HgLI_2$, D: $HgL(SCN)_2$, E: $HgL(NO3)_2$ and F:

$HgL(N_3)_2$, La, P, N and L lanes including La: ladder, P: (Pure DNA), N: (DNA+H_2O_2), and L: Schiff base ligand.

3.10. Cytotoxicity assessment

Cytotoxicity test for the ligand and its mercury halide complexes against the prostate cancer cells (PC3) line was performed as compared with cisplatin. The values of IC_{50}, an image of the PC3 cell line after treatment with the test compounds and the cell viability percentage plots of them are reported/ illustrated in Table 10 and fig. 9 and fig.2S (in supplementary file), respectively. As shown in fig. 9 and as compared with the control image(untreated), 24 hours after treatment of PC3 cell line with the tested compounds, the changes such as enlargement, protrusions on the cell surface and membrane contractions of cancer cells are observed confirming cytotoxicity of the compounds.

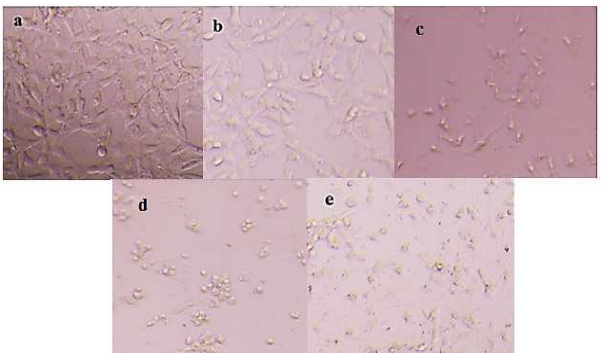

Fig. 9. Image of PC3 cells 24 hours after treatment with synthesized compounds; a: Control, b: Ligand, c: $HgLCl_2$, d: $HgLBr_2$, e: $HgLI_2$.

Among the tested compounds, mercury complexes were more effective than free ligand and among the complexes; mercury iodide complex was the most effective one. IC_{50} is a concentration of the drug that inhibits 50% of cell proliferation as compared with negative control. Generally, the higher concentrations are not used as cytotoxic doses in treatment but in the treatment of the disease, drug doses are used that have the highest effect with the least amount of damage to healthy cells. This dose is used as an effective drug dose. It is obvious that the values of drug dose vary for different cells. In current study, doses less than 70% of the IC_{50} were used as a drug doses that have been determined according to the behavior of treated cells and their morphological characteristics. Based on the IC_{50} and effective drug doses evaluated (table 10) regarding the cell vitality percentage plots (Fig.2S in supplementary file), cytotoxicity effects of the test compounds obey from the trend of $HgLI_2$>$HgLBr_2$>$HgLCl_2$>free ligand. It is noteworthy to know that mercury complexes have acceptable toxicity against PC3 as compared with cisplatin. The observed trend for these compounds may be proposed based on lipophilicity trend of the complexes so that the less polarity and therefore more lipophilicity lead to more activity as found in our conditions.

Table 10: IC_{50} values (μg/mL) of the ligand and its mercury complexes against PC3 cell line as compared with cisplatin.

Compounds	Ligand	$HgLCl_2$	$HgLBr_2$	$HgLI_2$	Cisplatin
IC_{50}	45.83	19.53	18.93	11.53	5.82
Effective drug dose	32.08	13.67	13.25	8.07	4.07

Nitric oxide level measurement is another common method for cytotoxicity evaluation. Nitric oxide is a lipophilic physiological messenger with high diffusion capacity and a short half-life that regulates many physiological responses such as vasodilation, cellular respiration, migration, immunity and apoptosis [62, 63]. Detection of nitric oxide was performed using the Griess method [62]. After 24 hours of treatment of PC3 cells with synthesized compounds, the amount of NO produced by these cells was measured. According to the obtained results, cisplatin not only did not inhibit NO production but also increased its production with respect to control test (untreated). It is to be noted that the titled compounds also increase the production of nitric oxide in PC3 cancer cells but the production of NO by the test compounds was lower than cisplatin (Fig. 10). Though according to Lennon et al studies, chemotherapeutic drug compounds such as cisplatin increase the amount of NO [64], which is consistent with the results obtained. Fortunately, the ligand and its mercury complexes have similar function with cisplatin as stranded in our conditions. Among the compounds, in agreement with previous method, mercury iodide complex had more cytotoxicity than other compound and, the ligand, mercury bromide and mercury chloride complexes are at the next order in cytotoxicity point of view under current conditions.

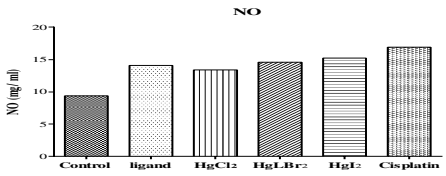

Fig.10. Evaluation of produced Nitric oxide by PC3 cells treated with ligand and mercury complexes.

3.11. Antioxidant activity

3.11.1. DPPH method

In the DPPH method, the amount of absorbance at characteristic wavelength indicates the amount of

present DPPH, so that more absorbance indicates the lower activity of antioxidant in the removal of free radicals. Accordingly, all the synthesized compounds at various concentrations were subjected to this test to evaluate their antioxidant potency. The results have been illustrated as bar graphs at fig.11 as % inhibition of DPPH (DPPH scavenging activity) versus compounds at various concentrations (µg/mL). Moreover evaluated values of IC_{50} and AEAC in µg/mL have been listed in table 11. As shown in fig. 11, by increasing the concentration of synthesized compounds, DPPH radicals are strongly inhibited (Fig.11). Regarding to the DPPH radicals scavenging activity, IC_{50} and AEAC values, the best antioxidant effect was related to the $HgL(SCN)_2$ complex (IC_{50} = 149.36µg/mL) and the lowest activity related to ligand (IC_{50}= 282.12 µg/mL) as compared with ascorbic acid as standard. It suggested that the ligand is electron source for antioxidant activity of the compounds. After coordination of the ligand to mercury center, its reduction potency may be affected depending on electron density changing on the ligand surface. Naturally an increase in electron density on the ligand surface increases antioxidant activity of the compound and vice versa. Accordingly, it can be said in mercury thiocyanate complex, S-coordinated thiocyanate send notable electron density on mercury(II) and indirectly on the ligand molecular orbitals leading to more reduction potency of DPPH or antioxidant activity than other tested compounds.

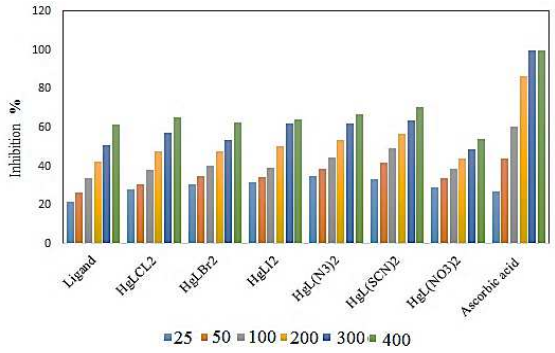

Fig. 11. DPPH scavenging activity (as inhibition %) of the Ligand, $HgLCl_2$, $HgLBr_2$, $HgLI_2$, $HgL(N_3)_2$, $HgL(SCN)_2$, $HgL(NO_3)_2$ and Ascorbic acid at 25, 50, 100, 200, 300 and 400 µg/mL.

3.11.2. FRAP method

Antioxidant potential calculated by the FRAP method is measured based on the ability of the antioxidant to reduce (Fe(III)-TPTZ) complex to the (Fe(II)-TPTZ) with an intensive blue color [65]. According to the obtained results that have been illustrated as bar graphs as FRAP concentration (µg/mL) versus compounds at definite concentration (as mentioned in experimental section) in fig.12, it was found that all the synthesized compounds exhibit antioxidant activity. Among them, the $HgL(N_3)_2$ complex showed the best antioxidant activity meanwhile $HgLCl_2$ complex has the lowest activity as compared with other compounds.

Table 11: IC_{50} and AEAC (µg/mL) values of the ligand and its mercury complexes.

Compounds	Ligand	$HgLCL_2$	$HgLBr_2$	$HgLI_2$	$HgL(N_3)_2$	$HgL(SCN)_2$	$HgL(NO_3)_2$	Ascorbic acid
IC_{50} (µg/mL)	282.12	233.31	240.97	210.43	177.90	149.367	218.94	70.98
AEAC(µg/mL)	251.60	304.23	294.57	337.315	399.01	475.22	324.21	-

In overall view, the antioxidant activity for the ligand and its complexes are arranged in the following order:

$HgL(N_3)_2$> $HgLBr_2$> $HgLI_2$ ~ $HgL(SCN)_2$> $HgL(NO_3)_2$> $HgLCl_2$> Ligand

Based on the DPPH method, it was expected that the mercury halide especially mercury iodide or mercury thiocyanate complex would be more antioxidant active if the outer sphere redox reaction was the main mechanism just similar to interaction between the complexes and DPPH but practically $HgL(N_3)_2$ was found the strongest antioxidant. To explain the observed results, inner-sphere redox reaction mechanism using the azide anion as bridging ligand between the iron(II) complex and mercury azide complex may be suggested. Except for this compound, the antioxidant activities trend of the other complexes may be discussed similarly to that was mentioned in the section of DPPH method.

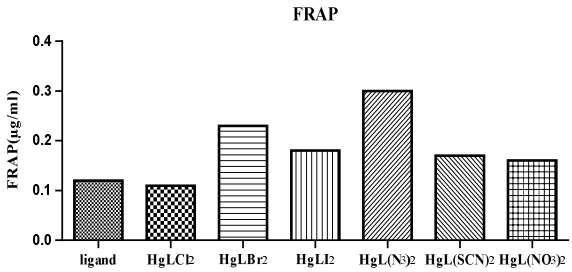

Fig. 12. FRAP (Ferric reducing-antioxidant power) of the Schiff base ligand and its Hg(II) complexes.

4. Conclusion

In this study, a new N_2O_2-Schiff base ligand and its new mercury(II) complexes with the general formula of $HgLX_2$ (X= Cl^-, Br^-, I^-, NO_3^-, N_3^-, and SCN^-) were

synthesized and characterized by physical and spectral techniques such as NMR, IR, UV, molar conductivity, thermal analysis, and melting point. Molecular conductivity in the range of 0.70 to 26 $cm^2\Omega^{-1}mol^{-1}$ confirmed the non-electrolyte character for all mercury complexes. Thermal decomposition analysis showed that the synthesized compounds are decomposed via 2-3 steps. Moreover, some thermo-kinetic activation parameters such as ΔS^*, ΔH^*, ΔG^*, E^*, and A^* were calculated based on Coats-Redfern equation. Positive values of enthalpy and Gibbs free energy changes of the decomposition processes at all steps confirmed the endothermic character for them. The antibacterial activities of the mentioned compounds revealed that the ligand had the lowest antibacterial activity. Evaluation of DNA cleavage potency showed that the mercury complexes were more efficient than free ligand. Cytotoxicity effects of ligand and its mercury complexes against PC3 cell line were evaluated by MTT and nitric oxide concentration level as compared with cisplatin as a positive control. According to the results, the $HgLI_2$ complex showed higher proliferative inhibitory effect than ligand and other mercury complexes. Finally, the antioxidant activities of the ligand and mercury complexes were investigated by the DPPH and FRAP methods. Regarding to both methods, all of the synthesized compounds showed good antioxidant activity meanwhile the mercury complexes had a better antioxidant potency than the free ligand.

Acknowledgement- Partial support of this work by Yasouj University is appreciated.

References

[1] R. Cavicchioli, Wi. J. Ripple, K. N. Timmis, F. Azam, L. R. Bakken, M. Baylis, M. J. Behrenfeld, A. Boetius, P. W. Boyd, A. T. Classen, T. W. Crowther, R. Danovaro, C. M. Foreman, J. Huisman, D. A. Hutchins, J. K. Jansson, D. M. Karl, B. Koskella, D. B. M. Welch, J. B. H. Martiny, M. A. Moran, Vi. J. Orphan, D. S. Reay, J. V. Remais, V. I. Rich, B. K. Singh, L. Y. Stein, F. J. Stewart, M. B. Sullivan, M. J. H. van Oppen, S. C. Weaver, E. A. Webb, N. S. Webster, Scientists' warning to humanity: microorganisms and climate change, *Nat. Rev. Microb. 17(*2019) 569-586.

[2] K. Buchacz, B. Lau, Y. Jing, R. Bosch, A. G. Abraham, M. J. Gill, M. J. Silverberg, J. J. Goedert, T. R. Sterling, K. N. Althoff, J. N. Martin, G. Burkholder, N. Gandhi, H. Samji, P. Patel, A. Rachlis, J. E. Thorne, S. Napravnik, K. Henry, A. Mayor, K. Gebo, S. J. Gange, R. D. Moore, J. T. Brooks, Incidence of AIDS-Defining Opportunistic Infections in a Multicohort Analysis of HIV-infected Persons in the United States and Canada, 2000-2010, *J. Infect. Dis.* 214(2016) 862-872.

[3] D. Salamon, T. Gosiewski, A. Krawczyk, A. Sroka-Oleksiak, M. Duplag, K. Fyderek, K. Kowalska-Duplaga, Quantitative changes in selected bacteria in the stool during the treatment of Crohn's disease. *Adv. Med. Sci. 65* (2020) 348-353.

[4] L. C. B. Rodrigues, A. F. Guimaraes, I. S. de Oliveira, P. H. M. de Sousa, R. M. de Castro Romanelli, F. M. Kakehasi, K. E. de Sá Rodrigues, Acute invasive fungal rhinosinusitis in pediatric patients with oncohematological diseases. *Hematol. Transfus. Cell Ther.* 44(2022) 32-39.

[5] P. G. Pappas, C. A. Kauffman, D. R. Andes, C. J. Clancy, K. A. Marr, L. Ostrosky-Zeichner, A. C. Reboli, M. G. Schuster, J. A. Vazquez, T. J. Walsh, T. E. Zaoutis, J. D. Sobel, Clinical Practice Guideline for the Management of Candidiasis: 2016 Update by the Infectious Diseases Society of America. *Clin. Infect. Dis.62(*2016) e1-50.

[6] T. Sangeetha, C. P. Rajneesh, W.-M. Yan, Integration of microbial electrolysis cells with anaerobic digestion to treat beer industry wastewater. In R. Abbassi, A. K. Yadav, F. Khan, V. Garaniya, Integrated Microbial Fuel Cells for Wastewater Treatment, Book Published by Elsevier, (2020) 313-346.

[7] C. Seiler, T. U. Berendonk, Heavy metal driven co-selection of antibiotic resistance in soil and water bodies impacted by agriculture and aquaculture. *Front. Microb.* 3 (2012) 399-408.

[8] A. Arunadevi, N. Raman, Biological response of Schiff base metal complexes incorporating amino acids – a short review. *J. Coord. Chem.* 73(2020) 2095-2116.

[9] S. Zhu, S. Xu, W. Jing, Z. Zhao, J. Jiang, Synthesis and Herbicidal Activities of p-Menth-3-en-1-amine and Its Schiff Base Derivatives. *J. Agric. Food Chem.* 64(2016) 9702–9707.

[10] G. Valarmathy, R. Subbalakshmi, R. Sumathi, R. Renganathan, Synthesis of Schiff base ligand from N-substituted benzenesulfonamide and its complexes: Spectral, thermal, electrochemical behavior, fluorescence quenching, in vitro-biological and in-vitro cytotoxic studies. *J. Mol. Struct.* 1199 (2020) 127029.

[11] S. Yu, Y. Wang, S. Wang, J. Zhu, S. Liu, The Antioxidant Activity and Catalytic Mechanism of Schiff Base Diphenylamines at Elevated Temperatures. *Ind. Eng. Chem. Res.*59 (2020) 1031-1037.

[12] Z. Saedi, E. Hoveizi, M. Roushani, S. Massahi, M. Hadian, K. Salehi, Synthesis, characterization, anticancer properties and theoretical study of asymmetrical Cd (II) N2-Schiff base complexes. *J. Mol. Struct.* 1176(2019) 207-216.

[13] W. H. Mahmoud, R.G. Deghadi, G.G. Mohamed, Novel Schiff base ligand and its metal complexes with some transition elements. Synthesis, spectroscopic, thermal analysis, antimicrobial and in vitro anticancer activity. *App. Organomet. Chemi. 30(*2016) 221-230.

[14] A. D. M. Mohamad, E. R. El-Shrkawy, M. F. I. Al-Husseind, M. S. S. Adam, Water-soluble Cu (II)-complexes of Schiff base amino acid derivatives as biological reagents and sufficient catalysts for oxidation reactions. *J. Taiwan Inst. Chem. Eng.113(* 2020) 27-45.

[15] M. Manimohan, R. Paulpandiyan, S. Pugalmani, M. A. Sithique, Biologically active novel N, N, O donor tridentate water soluble hydrazide based O-carboxymethyl chitosan Schiff base Cu (II) metal complexes: Synthesis and characterization. *Int. J. boil. Macromol.* 163 (2020) 801-816.

[16] Z. Shariatinia, Pharmaceutical applications of chitosan. *Adv. Colloid Interface Sci.* 263(2018) 131-194.

[17] L. Li, Z. Li, K. Wang, S. Zhao, J. Feng, J. Li, P. Yang, Y. Liu, L. Wang, Yongqiang Li, H. Shang, Q. Wang, Design, Synthesis, and Biological Activities of Aromatic Gossypol Schiff Base Derivatives. *J. Agric. Food Chem. 62(*2014) 11080-11088.

[18] R. Cordeiroa, M. Kachroo, Synthesis and biological evaluation of anti-tubercular activity of Schiff bases of 2-Amino thiazoles. *Bioorga. Med. Chem. Lett.* 30(2020) 127655.

[19] Z. Akbari, M. Montazerozohori, S. J. Hoseini, R. Naghiha, P. Hayati, G. Bruno, A. Santoro, J. M. White, Synthesis, crystal structure, Hirshfeld surface analyses, antimicrobial activity, and thermal behavior of some novel nanostructure hexa-coordinated Cd(II) complexes: Precursors for CdO nanostructure. *App. Organomet. Chem.* 36 (2021) e6181.

[20] V. Bressi; Z. Akbari, M. Montazerozohori, A. Ferlazzo, D. Iannazzo, C. Espro, G. Neri, On the Electroanalytical Detection of Zn Ions by a Novel Schiff Base Ligand-SPCE Sensor. *Sensors* 22(2022) 900(1-15).

[21] R. Eshaghi Malekshah, F. Shakeri, A. Khaleghian, M. Salehi, Developing a biopolymeric chitosan supported Schiff-base and Cu (II), Ni (II) and Zn (II) complexes and biological evaluation as pro-drug. Int. *J. Biol. Macromol.* 152 (2020) 846-861.

[22] W. Zhang, T. Shi, G. Ding, D. Punyapitak, J. Zhu, D. Guo, Z. Zhang, J. Li, Y. Cao, Nanosilica Schiff-Base Copper(II) Complexes with Sustainable Antimicrobial Activity against Bacteria and Reduced Risk of Harm to Plant and Environment. *ACS Sustain. Chem. Eng.* 5(2017) 502-509.

[23] W. H. Mahmoud, R. G. Deghadi, G. G. Mohamed, Metal complexes of ferrocenyl-substituted Schiff base: Preparation, characterization, molecular structure, molecular docking studies, and biological investigation, *J. Organomet. Chem.* 917(2020) 121113.

[24] M. L. Low, L. Maigre, P. Dorlet, R. Guillot, J.-M. Pagès, K. A. Crouse, C. Policar, N. Delsuc, Conjugation of a new series of dithiocarbazate Schiff base copper (II) complexes with vectors selected to enhance antibacterial activity. *Bioconjug. Chem.* 25(2014) 2269-2284.

[25] Y.-T. Liu, J. Sheng, D.-W. Yin, H. Xin, X.-M. Yang, Q.-Y. Qiao, Z.-J. Yang, Ferrocenyl chalcone-based Schiff bases and their metal complexes: Highly efficient, solvent-free synthesis, characterization, biological research. *J. Organomet. Chem.* 856(2018) 27-33.

[26] X. Liu, C. Manzur, N. Novoa, S. Celedon, D. Carrillo, J. -R. Hamon, Multidentate unsymmetrically-substituted Schiff bases and their metal complexes: Synthesis, functional materials properties, and applications to catalysis. *Coord. Chem. Rev.* 357(2018) 144-172.

[27] J. Szklarzewicz, A. Jurowska, D. Matoga, K. Kruczała, G. Kazek, B. Mordyl, J. Sapa, M. Papiez, Synthesis, coordination properties and biological activity of vanadium complexes with hydrazone Schiff base ligands. *Polyhedron* 185(2020) 114589.

[28] E. S. Mousa, W. H. Mahmoud, Spectroscopic, textural, electrical and magnetic properties of antimicrobial nano Fe (III) Schiff base complex. *App. Organomet. Chemi.* 33(2019) e4844.

[29] A. Frei, A. P. King, G. J. Lowe, A. K. Cain, F. L. Short, H. Dinh, A. G. Elliott, J. Zuegg, J. J. Wilson, M. A. T. Blaskovich, Nontoxic Cobalt(III) Schiff base complexes with broad-spectrum antifungal activity. *Chem. Eur. J.* 26(2020) 1-10.

[30] T. Chowdhury, S. Dasgupta, S. Khatua, K. Acharya, D. Das, Executing a Series of Zinc (II) Complexes of Homologous Schiff Base Ligands for a Comparative Analysis on Hydrolytic, Anti-oxidant and Anti-bacterial Activities. *ACS App. Biomat.* 3(2020) 4348-4357.

[31] A. Kapila, M. Kaur, H. Kaur, Organotin(IV) complexes of tridentate (O,N,O) Schiff base ligand: computational, spectroscopic and biological studies. *Mat. Today: Proc.* 40(2020) S102-S106.

[32] M. Gillard, J. Weynand, H. Bonnet, F. Loiseau, A. Decottignies, J. Dejeu, E. Defrancq, B. Elias, Flexible RuII Schiff Base Complexes: G-Quadruplex DNA Binding and Photo-Induced Cancer Cell Death. *Chem. Eur. J.* 26(2020) 13849-13860.

[33] M. Bian, X. Wang, Y. Sun, W. Liu, Synthesis and biological evaluation of gold(III) Schiff base complexes for the treatment of hepatocellular carcinoma through attenuating TrxR activity. *Eur. J. Med. Chem.*193 (2020) 112234.

[34] S. Silvano, C. F. Carrozza, A. R. de Angelis, I. Tritto, L. Boggioni, S. Losio, Synthesis of Sulfur-rich Polymers: Copolymerization of Cyclohexene Sulfide and Carbon Disulfide Using Chromium Complexes. *Macromol.* 53(2020) 8837-8846.

[35] A. Sarkar, A. Chakraborty, T. Chakraborty, S. Purkait, D. Samanta, S. Maity, D. Das, A Chemodosimetric Approach for Fluorimetric Detection of Hg2+ Ions by Trinuclear Zn(II)/Cd(II) Schiff Base Complex: First Case of Intermediate Trapping in a Chemodosimetric Approach. *Inorg. Chem.* 59(2020) 9014-9028.

[36] G. Mahmoudi, M. Servati Gargari, F. Akbari Afkhami, C. Lampropoulos, M. Abedi, S. A. Corrales, A. A. Khandar, J. Mague, D. Van Derveer, B. K. Ghoshg, A. Masummi, Mercury (II) coordination complexes bearing Schiff base ligands: What affects their nuclearity and/or dimensionality. *Polyhedron* 93(2015) 46-54.

[37] R.K. Dubey, P. Baranwal, A.K. Jha, Zinc (II) and mercury (II) complexes with Schiff bases: syntheses, spectral, and structural characterization. *J. Coord. Chemi.* 65(2012) 2645-2656.

[38] A. Tamayo, B. Pedras, C. Lodeiro, L. Escriche, J. Casabo, J.L. Capelo, B. Covelo, R. Kivekas, R. Sillanpaa, Exploring the interaction of mercury(II) by N(2)S(2) and NS(3) anthracene-containing macrocyclic ligands: photophysical, analytical, and structural studies. *Inorg. Chem.* 46(2007) 7818-7826.

[39] P. Parameshwara, J. Karthikeyan, A.N. Shetty, P. Shetty, Quantitative complexometric determination of mercury(II) in synthetic alloys and complexes using 2-thiazolinethiol as a masking agent, *J. Iran. Chem. Soc.* 3(2006) 168.

[40] S. A. Musavi, M. Montazerozohori, M. Nasr-Esfahani, R. Naghiha, M. Montazer Zohour, Nano-structure zinc and cadmium azide and thiocyanate complexes: Synthesis, characterization, thermal, antimicrobial and DNA interaction. *Bulg. Chem. Commun.* 48(2016) 209 - 218.

[41] P. Kumar, A. Nagarajan, P.D. Uchil, Analysis of Cell Viability by the alamarBlue Assay. *Cold Spring Harb. Protoc.* 2018 (2018) 29858336.

[42] K. M. Miranda, M. G. Espey, D. A. Wink, A rapid, simple spectrophotometric method for simultaneous detection of nitrate and nitrite. *Nitric Oxide* 5(2001) 62-71.

[43] A. A. Al-Amiery, A. A. H. Kadhum, A. B. Mohamad, Antifungal and Antioxidant Activities of Pyrrolidone Thiosemicarbazone Complexes. Bioinorg. Chem. Appl. 2012(2012) 795812.

[44] I. F. F. Benzie, J. J. Strain, The ferric reducing ability of plasma (FRAP) as a measure of "antioxidant power": the FRAP assay. *Anal. Biochem.* 239(1996) 70–76.

[45] I. Ali, W. A. Wani, K. Saleem, Empirical Formulae to Molecular Structures of Metal Complexes by Molar Conductance. Synth. React. Inorg. Met.-Org. Chem 43(2013) 1162-1170.

[46] F. K. Ommenya, E. A. Nyawade, M. Andala, J. Kinyua, Synthesis, Characterization and Antibacterial Activity of Schiff Base, 4-Chloro-2-{(E)-[(4-Fluorophenyl)imino]methyl}phenol Metal (II) Complexes, *Journal of Chemistry, 2020(*2020) 1745236(1–8).

[47] R. S. Bhaskar, C. A. Ladole, N. G. Salunkhe, J. M. Barabde, A. S. Aswar, Synthesis, characterization and antimicrobial studies of novel ONO donor hydrazone Schiff base complexes with some divalent metal (II) ions. *Arab. J. Chem.* 13(2020) 6559-6567.

[48] A. D. Kulkarni, S. A. Patil, P. S. Badami, Electrochemical Properties of some Transition Complexes: Synthesis, Characterization and In-vitro antimicrobial studies of Co(II), Ni(II), Cu(II), Mn(II) and Fe(III) Complexes. *Int. J. Electrochem. Sci.* 4(2009) 717-729.

[49] M. H. E. Chan, K. A. Crouse, M. I. M. Tahir, R. Rosli, N. Umar-Tsafe, A. R. Cowley, Synthesis and characterization of cobalt (II), nickel (II), copper (II), zinc (II) and cadmium (II) complexes of benzyl N-[1-(thiophen-2-yl) ethylidene] hydrazine carbodithioate}nickel(II), *Polyhedron* 27(2008) 1141-1149.

[50] M. Montazerozohori, A. Nazaripour, A. Masoudiasl, R. Naghiha, M. Dusek, M. Kucerakova, Antimicrobial activity, DNA cleavage, thermal analysis data and crystal structure of some new CdLX2 complexes: A supramolecular network, Mat. Sci. Eng.*:C* 55(2015) 462-470.

[51] M. Montazerozohori, S. Musavi, A. Masoudiasl, A. Hojjati, A. Assoud DFT study and crystal structure analysis of a new nano-structure five coordinated Hg(II) complex involving C–H···O, N···O and π···π interactions in a supra-molecular structure, *Spectrochim. Acta A* 147(2015) 139-150.

[52] A. Masoudiasl, M. Montazerozohori, R. Naghiha, A. Assoud, P. McArdle, M. S. Shalamzari, Synthesis, X-ray crystal structures and thermal analyses of some new antimicrobial zinc complexes: New configurations and nano-size structures. *Mat. Sci. Eng.:C* 2016, 61, 809-823.

[53] M. Montazerozohori, S. M. Jahromi, A. Naghiha, Thermal analyses data and antimicrobial screening of some new nano-structure five coordinated cadmium complexes. *J. Ind. Eng. Chem.* 22(2015) 248-257.

[54] M. Montazerozohori, S. M. Jahromi, A. Masoudiasl, P. McArdle, Nano structure zinc (II) Schiff base complexes of a N3-tridentate ligand as new biological active agents: Spectral, thermal behaviors and crystal structure of zinc azide complex. Spectrochim. Acta A 1382015) 517-528.

[55] N. Dharmaraj, P. Viswanathamurthi, K. Natarajan, Ruthenium(II) complexes containing bidentate Schiff bases and their antifungal activity, *Trans. Met. Chem.* 26(2001) 105-109.

[56] M. Montazerozohori, S. Yadegari, A. Naghiha, S. Veyseh, Synthesis, characterization, electrochemical behavior, thermal study and antibacterial/antifungal properties of some new zinc(II) coordination compounds. *J. Ind. Eng. Chem.* 20*(*2014) 118-126.

[57] J. Yang, C. Lin, Z. Wang, *J. Lin,* $In(OH)_3$ and In_2O_3 Nanorod Bundles and Spheres: Microemulsion-Mediated Hydrothermal Synthesis and Luminescence Properties. *Inorg. Chem.* 45(2006) 8973–8979.

[58] A. W. Coats, J. Redfern, Kinetic Parameters from Thermogravimetric Data, *Nature.,* 201(1964) 68-69.

[59] G. Consiglio, I. P. Oliveri, S. Failla, S. Di Bella, Supramolecular Aggregation of a New Substituted Bis(salicylaldiminato)zinc(II) Schiff-Base Complex Derived from trans-1,2-Diaminocyclohexane, *Inorganics* 6 (2018)1-13.

[60] P. Maravalli, T. Goudar, Thermal and spectral studies of 3-N-methyl-morpholino-4-amino-5-mercapto-1,2,4-triazole and 3-N-methyl-piperidino-4-amino-5-mercapto-1,2,4-triazole complexes of cobalt(II), nickel(II) and copper(II). *Thermochim. Acta* 325(1999) 35-41.

[61] M. A. Goher, F. A. Mautner, B. Sodin, B. Bitschnau, Synthesis, spectral and structural characterization of three zinc (II) azide complexes with aminopyrazine, *J.Mol. Struct.* 879 (2008) 96-101.

[62] J. Muntané, A. J. De la Rosa, L. M. Marín, F. J. Padillo, Nitric oxide and cell death in liver cancer cells. *Mitochondrion.* 13(2013) 257-262.

[63] M. Jordi, M. Mata, Nitric oxide and cancer. *World J. Hepatol.* 27 (2010)) 337-344.

[64] S. V. Lennon, S. J. Martin and T. G. Cotter, Dose-dependent induction of apoptosis in human tumour cell lines by widely diverging stimuli. *Cell Prolif.* 24(1991) 203-214.

[65] I. F. F. Benzie, J. J. Strain, The ferric reducing ability of plasma (FRAP) as a measure of “antioxidant power”: the FRAP assay. *Anal. Biochem.* 239 (1996) 70-76.